2009

Dynamical Fluctuations in Dense Granular Flows

Emily Gardel
Smith College

E. Seitaridou
Smith College

Kevin Facto
University of Massachusetts Amherst

E. Keene
Smith College

K. Hattam
Smith College

See next page for additional authors

PHILOSOPHICAL TRANSACTIONS OF THE ROYAL SOCIETY A

Phil. Trans. R. Soc. A (2009) **367**, 5109–5121
doi:10.1098/rsta.2009.0189

Dynamical fluctuations in dense granular flows

By Emily Gardel[1], E. Seitaridou[1], Kevin Facto[2], E. Keene[1], K. Hattam[1], Nalini Easwar[1] and Narayanan Menon[2,*]

[1]*Department of Physics, Smith College, Northampton, MA 01063, USA*
[2]*Department of Physics, University of Massachusetts, Amherst, MA 01003, USA*

We have made measurements of force and velocity fluctuations in a variety of dense, gravity-driven granular flows under flow conditions close to the threshold of jamming. The measurements reveal a microscopic state that evolves rapidly from entirely collisional to largely frictional, as the system is taken close to jamming. On coarse-grained time scales, some descriptors of the dynamics—such as the probability distribution of force fluctuations, or the mean friction angle—do not reflect this profound change in the micromechanics of the flow. Other quantities, such as the frequency spectrum of force fluctuations, change significantly, developing low-frequency structure in the fluctuations as jamming is approached. We also show evidence of spatial structure, with force fluctuations being organized into local collision chains. These local structures propagate rapidly in the flow, with consequences far away from their origin, leading to long-range correlations in velocity fluctuations.

Keywords: granular flow; jamming; force chains

1. Introduction

The description of a dense equilibrium fluid is a difficult problem in condensed matter physics. In the case of a dense granular fluid, these difficulties are compounded by the fact that particle motions do not originate in thermal fluctuations, but are due to small-scale fluctuations generated by large-scale external forces acting on the material. Furthermore, interparticle interactions are dissipative and can occur in one of two ways, either by inelastic collisions or by frictional contacts between particles.

There is a large body of work in which the effort is to describe the rheology of granular flows in terms of continuum constitutive relations, from measurements of macroscopic flow profiles (Ertas & Halsey 2002; GDR MiDi 2004; Forterre & Pouliquen 2008). The approach taken in the experiments described in this paper is different. We will describe direct measurements of microscopic fluctuations in local forces and local velocity fluctuations in a variety of flow geometries. The goal is thus to build up an overall microscopic picture of the fluid state. In particular,

*Author for correspondence (menon@physics.umass.edu).

One contribution of 12 to a Discussion Meeting Issue ‘Colloids, grains and dense suspensions: under flow and under arrest’.

we follow the evolution of this microscopic state as the external conditions are varied until the material jams, and is no longer able to flow. When close to jamming, is there something in the internal state of the fluid that foretells the impending arrest into a jammed state?

In this paper, we present experimental measurements characterizing the two kinds of micromechanics—collisional or frictional—supported by dense grain flows. In some geometries, collisional mechanics dominates almost to the point of jamming. In §2 we discuss the conditions under which you get one or the other flow. In §3 we quantify the fluctuations in each regime, and show that there is a broad distribution of forces in the fluid state, just as in the jammed state of granular materials (Mueth *et al.* 1998). Finally, we show in §4 that force fluctuations with relatively local correlations can lead to correlated flow over long length scales, and that these length scales increase as one approaches the jamming transition.

2. Experiments on gravity-driven flows

The flow geometries chosen for our experiments are all vertical, gravity-driven flows. These mimic the industrially significant situations of hopper flow and silo drainage.

We note that these are different from sheared systems (Losert *et al.* 2000; Mueth *et al.* 2000) or vibrated systems (Knight *et al.* 1997) in that the energy input to the system is not from a boundary. As a result, these flows are also relatively homogeneous. There are, of course, gradients near the confining walls of the flow since the walls play a crucial role in transforming the homogeneous energy input into relative motions of the particles, but these shear zones near the walls typically extend a few particle diameters before matching up to the bulk flow (Pouliquen & Gutfraind 1996). The bulk flow is often described as a ‘plug flow’, in that the flow velocity is almost uniform across a section of the flow. However, it is important to realize that particles in this plug are directly driven by gravity, and that, while the edges of the system are crucial in generating particle fluctuations, these fluctuations are not confined to the shear zones. (In this sense, this geometry may be different from the ‘toothpaste’ colloidal geometry of the Edinburgh group; Isa *et al.* 2007.) Finally, these are not fixed-volume geometries, and the density regulates itself under a given flow condition, becoming denser as jamming is approached. However, unlike in flows down an inclined plane (Pouliquen 1999; Silbert *et al.* 2001), there is little access to a free surface, and the density in the system is relatively homogeneous at any given flow condition.

In figure 1, we show four different flow geometries employed in our experiments. Two of these (figure 1*a*,*b*) are quasi-two-dimensional geometries in which the particles in the flow are sandwiched between plates that are separated by $1.1d$, where d is the particle diameter. The other two (figure 1*c*,*d*) are fully three-dimensional geometries. In all cases, the granular flow is composed of monodisperse glass or steel spheres, with particle diameter in the range $d = 1$–3 mm. We study the kinematics of the flow by high-speed video imaging at frame rates of 400 to 8000 Hz; in the case of the three-dimensional flows, our observations are limited to the surface of the flow.

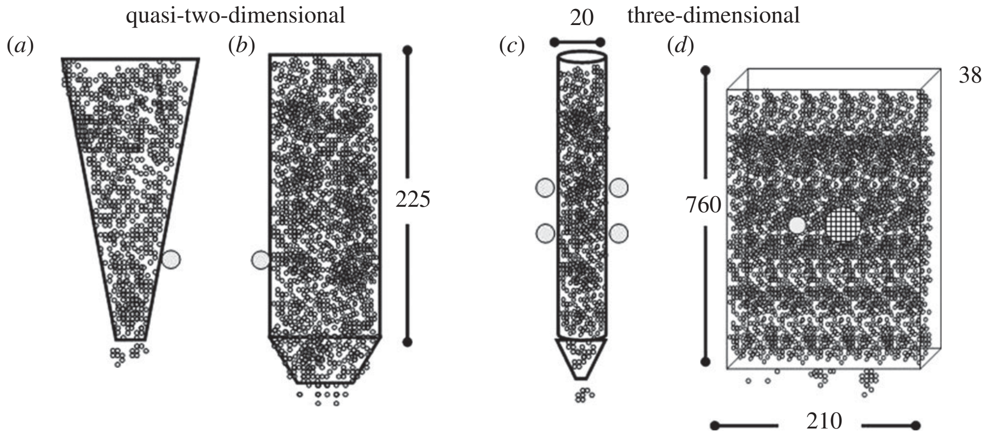

Figure 1. Four flow geometries with relevant sizes indicated in units of the particle diameter d. (a) Two-dimensional hopper with sidewall at 10° from the vertical. This is a steep angle, so that there are no dead zones in the hopper. (b) Two-dimensional silo. The width of the straight section of the silo can be varied from $6d$ to $30d$. (c) Three-dimensional cylindrical silo. (d) Three-dimensional channel with a rectangular cross-section. In all these flows, the flow velocity is controlled by changing the aperture a of the outlet. In (d), the outlet is a sieve with a series of holes. The grey circles indicate transducers sensitive only to normal forces; the active surface of each of these transducers accommodates only one sphere, and has a response time of approximately 10 μs. In (c), we have embedded four transducers whose separation and relative orientation can be varied. The larger hatched circle in (d) measures all three components of force, accommodates approximately 12 spheres on its surface and has a response time of approximately 25 μs.

All the flows are fed from a larger reservoir above the flow cell. The flow rate is varied by adjusting the diameter of the outlet while keeping all other dimensions fixed. The flows jam permanently when the linear dimension of the outlet is reduced to a few particle diameters. For the two-dimensional geometries, we are able to vary flow velocity by a factor of 8–10, while in the three-dimensional geometries, the dynamic range in velocity is about 25. While this was not the focus of any of our studies, the flow rates are consistent with the Beverloo correlation (Beverloo *et al.* 1961), namely, that the flow rate can be estimated by $Ca^{D-1}\sqrt{gha}$, the product of the outlet area and the velocity produced by falling freely under gravity from a height comparable to the linear size a of the outlet (C is a constant of order 1 that depends on the exit angle, grain shape and other parameters, and D is the spatial dimension).

We embed piezo-electric transducers (grey circles in figure 1) in the walls of the cells to measure the normal force exerted by the flow. These have a fast response time, shorter than the duration of a particle–wall collision (approx. 30–50 μs). The response to impulses was calibrated directly by collisions of particles with known impulses. In the three-dimensional flow in figure 1d, we also introduce a transducer with several crossed strain gauges that can measure all three components of the wall force. Data were taken from this transducer at a lower digitization rate of 25 kHz and then low-passed to the desired noise level.

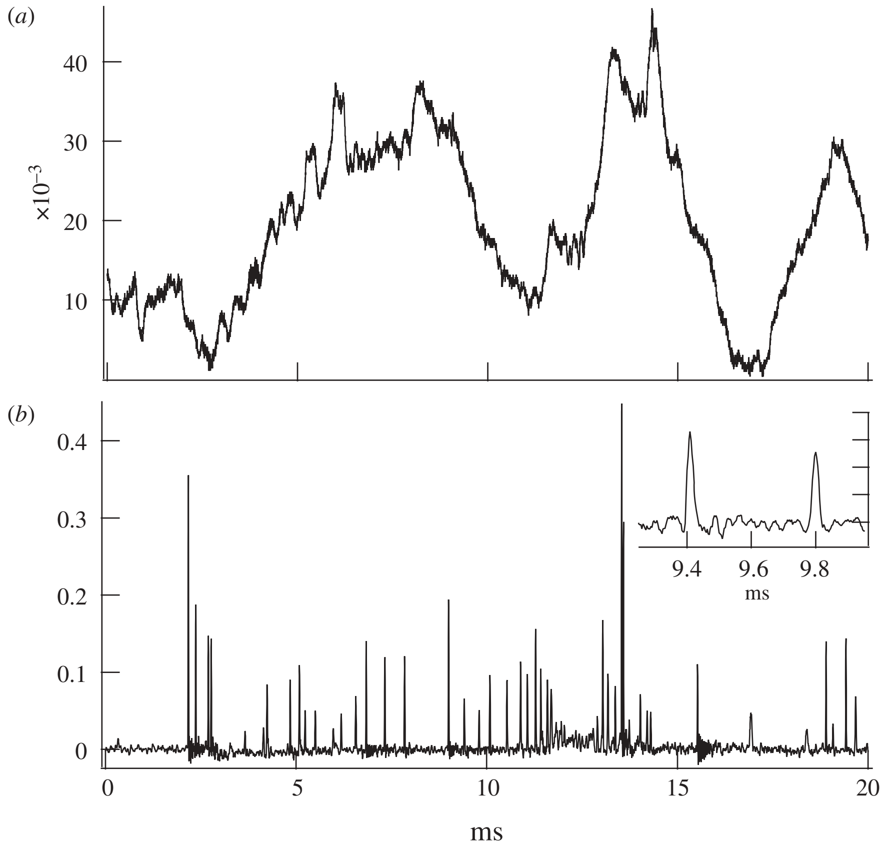

Figure 2. Time series of transducer output (arbitrary units) in the geometry of figure 1*c* for (*a*) a slow flow with $a = 4d$ and (*b*) a fast flow with $a = 10d$, where a is the diameter of the outlet. In the inset of (*b*) we show a magnified version of a small section of the trace to show that the collision is fully resolved at the digitization rate of 320 kHz.

3. Collisional and frictional regimes

In each one of the setups shown in figure 1, as the outlet is restricted to reduce the velocity, the mechanism of momentum transfer to the walls progresses from impulsive collisions to enduring contacts. We show this directly by showing time traces of the transducer voltage in figure 2 for the fastest and slowest flow rates that we were able to use in the setup of figure 1*c*. In figure 2*a*, the force on the wall is continuous and non-zero, whereas in figure 2*b*, the force trace consists of isolated collisions against the wall.

This remarkable evolution in the particle dynamics as one approaches jamming occurs with very little change in the density. This strong qualitative change in the mechanism of interaction is extremely difficult to discern using video measurements. Using a typical collision frequency of 2 kHz and a typical fluctuation velocity of $\delta v = 1\,\mathrm{cm\,s^{-1}}$, one obtains a mean free path, $s = 5\,\mu\mathrm{m}$. (Similar estimates have been obtained from diffusive wave scattering techniques; Menon & Durian 1997.) Thus, in order to resolve ballistic flight of a

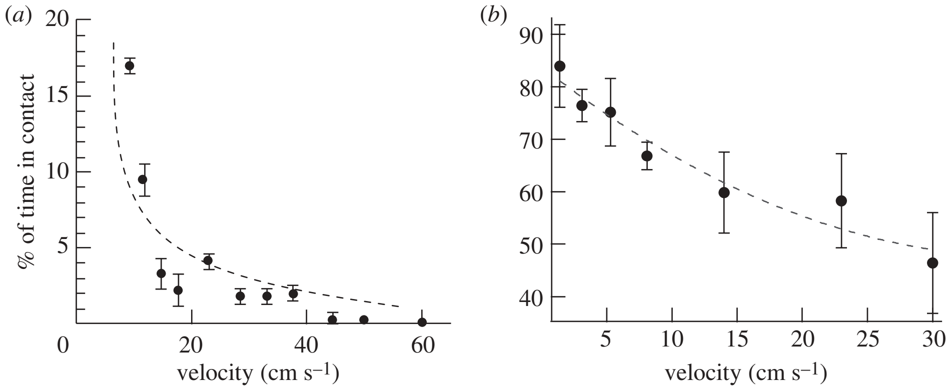

Figure 3. Percentage of the time when the transducer is in contact with a particle as a function of flow rate for (*a*) two-dimensional hopper and (*b*) three-dimensional silo geometries.

macroscopic sphere with $d \sim 1\,\mathrm{mm}$, a spatial resolution of approximately $1\,\mu\mathrm{m}$ is required, which is difficult to achieve with video microscopy of spheres in near-contact geometries.

The evolution from collisional to frictional interparticle dynamics is not a sharp transition, but a crossover that progresses continuously as one approaches jamming. A metric by which this crossover may be followed is the fraction of the time that the transducer is in contact with a particle. The percentage contact time is shown in figure 3 as a function of flow rate for the two-dimensional hopper (figure 1*a*) and three-dimensional silo (figure 1*c*) geometries. The lowest flow rate in both cases corresponds to the smallest outlet size for which the flow did not jam. As the figure shows, the percentage of contact time grows continuously, though the dependence on the flow rate is sharper in the two-dimensional hopper, where the flow remains largely collisional very close to the jamming threshold. In both these cases, this strong change in the momentum transfer mechanism occurs with very little change in packing fraction.

A richer characterization of the temporal fluctuations in the force is shown in figure 4, where we plot the power spectrum of the time series of the force for a series of flow rates approaching jamming, in the three-dimensional silo geometry. One feature that is obvious in the power spectra is a peak at high frequencies, corresponding to the duration of a single Hertzian collision of a sphere with a transducer. The amplitude of this collisional peak reduces as the flow rate decreases, consistent with our observation that the dynamics becomes more frictional. However, at frequencies lower than the collisional peak, there is a non-trivial variation of the power spectrum that cannot be described by a shift to longer time scales of the entire spectrum. The flow rates closer to jamming have much more low-frequency content than the predominantly collisional flows, and at the lowest frequencies, a small peak emerges at approximately 100 Hz.

The collisional-to-frictional crossover is qualitatively similar in all the geometries we discuss; however, quantitative details of the approach to frictional mechanics depend both on particle properties and on the flow geometry. In figure 5, we show power spectra in the two-dimensional silo geometry to illustrate the effect of change in particle property and system width.

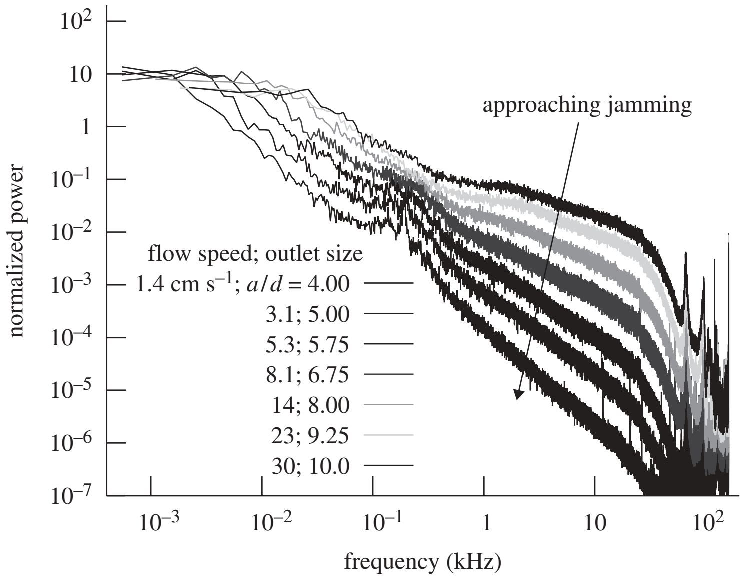

Figure 4. Power spectrum of the normal force delivered to the wall in the three-dimensional silo geometry. The curves for different flow rates are displaced vertically for clarity; and the key refers to the curves from bottom to top.

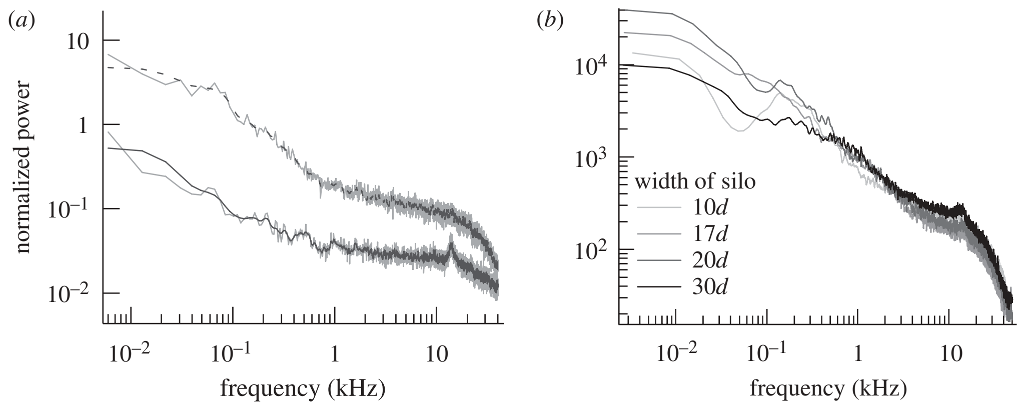

Figure 5. (a) Comparison of force power spectra taken at the same flow rate for glass and steel spheres in a two-dimensional silo geometry. The grey curves show the raw data, while the black curves are low-passed to improve the signal-to-noise ratio at higher frequencies. The collisional peak is apparent in the data for glass (full curve), but is absent for steel (dashed curve, displaced upward for clarity), which has a slightly lower coefficient of restitution. (b) Comparison of force spectra for varying widths of the silo.

4. Force distributions

In a steady, height-independent, flow, the average force at the wall does not change as a function of flow rate; the vertical force provided by a section of the wall supports the weight of the grains enclosed within that section, and this

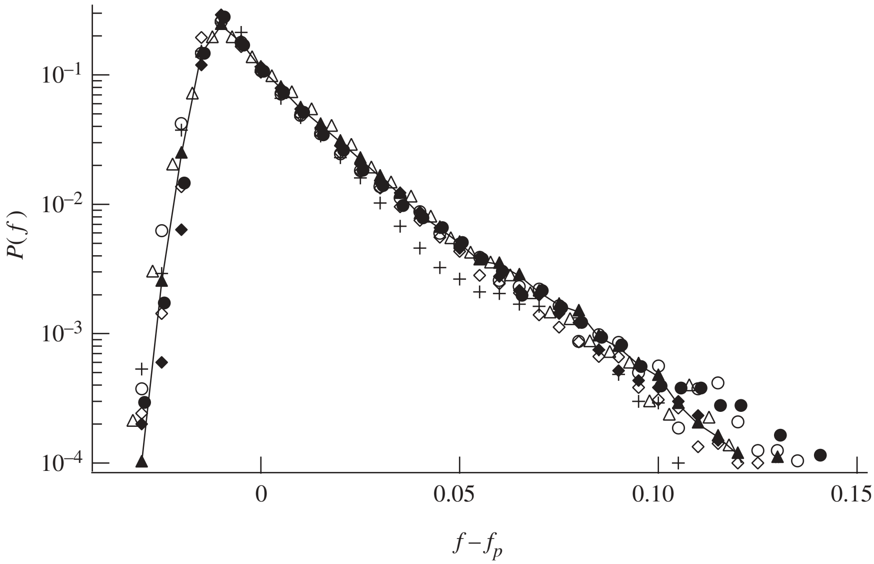

Figure 6. Probability distribution of force, $P(f)$, plotted for a range of flow rates in the three-dimensional silo geometry, against $f - f_\mathrm{p}$, where f_p is the force at which the distribution peaks. The force, f, is computed by time averaging the force over 0.25 ms, which is considerably longer than the duration of a single Hertzian collision, of about 30 μs, and is comparable to the mean time between collisions at the highest of these flow rates. The distribution is not sensitive to changes in the averaging time scale if this condition is satisfied. Outlet size, a/d: plus, 4; open triangle, 5; filled triangle, 5.75; open diamond, 6.75; filled diamond, 8; open circle, 9.25; filled circle, 10.

weight is independent of the flow rate except to the extent to which the density decreases slightly as the flow rate is increased. In this section, we explore the issue of whether the distribution of the force about this average changes. In Longhi *et al.* (2002), we studied the distribution of individual impulses in the limit of a nearly collisional flow. The distribution of impulses showed an exponential tail, which did not evolve with the flow rate.

In order to compare the forces across the collision–friction crossover, the forces must be time averaged at a time scale longer than the duration of a collision. The averaging time scale, however, must not be much longer than the autocorrelation time of the force trace in order not to average over independent samplings of the force. We show in figure 6 the probability distribution of force, $P(f)$, in the three-dimensional silo geometry. $P(f)$ shows no evolution even though the flow rates vary by a factor of 20. The tail of the distribution is exponential at all flow velocities, as has been found in static granular materials (Mueth *et al.* 1998). We had previously observed this in Longhi *et al.* (2002) in the two-dimensional silo geometry, where the dynamics is collisional almost until the jamming threshold. However, as shown in figure 6, this distribution remains unchanged even though the microscopic dynamics changes from collisional to frictional. Indeed, no evidence is seen of the approach to jamming in $P(f)$. Previous experiments and simulations show that the probability of low forces builds in $P(f)$ on the approach to jamming; however, we see no evidence of such a structure in the range that we are able to access experimentally.

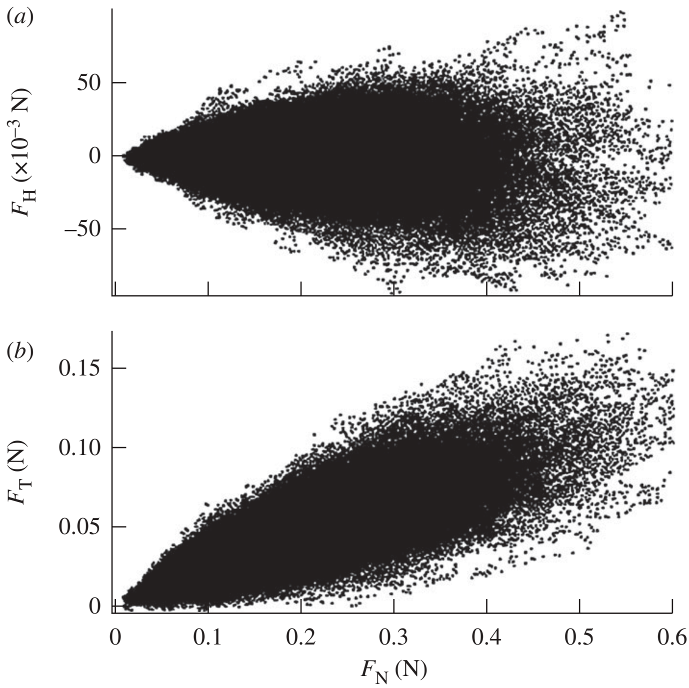

Figure 7. Scatter plots of force components: (*a*) F_{H}, horizontal force in the plane of the wall, and (*b*) F_T, tangential component of force, both plotted against F_{N}, the normal force against the wall. Plot (*b*) shows a well-defined frictional angle, $\tan^{-1}(F_{\mathrm{T}}/F_{\mathrm{N}})$.

We have also recently measured (K. Facto, T. J. Schicker & N. Menon 2009, unpublished data) all three components of the force at the walls of a three-dimensional channel (figure 1*d*), again over a range of flow velocities spanning a factor of approximately 25. Here, too, the distributions of all three force components remain unchanged over the entire range of velocities. As shown in the scatter plots of figure 7, the force components lie clustered in a narrow range defining a 'friction angle' at the wall. The friction angle is independent of the flow rate over this wide range of velocities. Indeed, even the fluctuations about this average friction angle are highly correlated, as shown in figure 8. Once again, the correlations appear to be completely independent of velocity over the entire range of flow rates.

Thus, the distribution of forces gives no indication of proximity to the jamming threshold even though there is substantial evolution in the temporal character of force fluctuations, and in the nature of the microscopic interaction between the particles.

5. Force and velocity correlations

The lack of indication of a jamming transition in the force distributions leads us to examine spatial correlations in force and velocity fluctuations for signatures of arrest. The search for a correlation length in the flowing state, or of any other

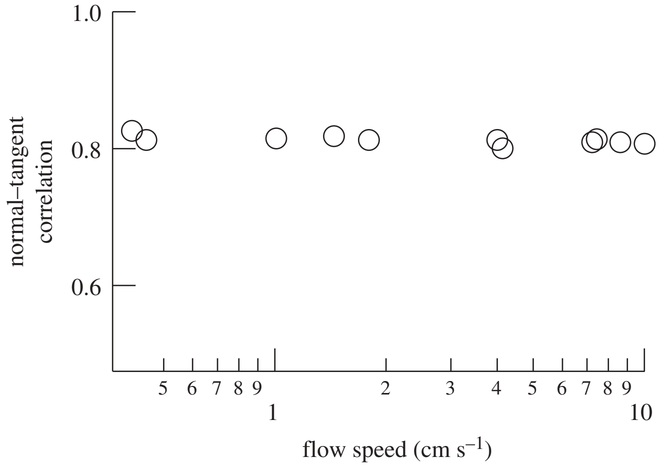

Figure 8. Coefficient of correlation between the normal and tangential force components, $\langle \delta F_{\mathrm{N}} \delta F_{\mathrm{T}} \rangle / \sqrt{\langle (\delta F_{\mathrm{N}})^2 \rangle \langle (\delta F_{\mathrm{T}})^2 \rangle}$, plotted against the flow velocity. Here δ denotes the fluctuation about the mean, and the angle brackets $\langle \quad \rangle$ denote a time average. The correlation is independent of flow rate, within the resolution of the experiment.

static signature of arrest, has of course been the subject of intense activity in the glass transition of molecular liquids, polymers and colloids. The arrest of a granular fluid may be different, partly because of its non-equilibrium nature, and also due to the fact that flow is often induced by a driving force that breaks spatial and temporal symmetries.

In previous work (Gardel *et al.* submitted), we have found evidence of strong spatial correlations between force and velocity fluctuations in the two-dimensional hopper geometry of figure 1*a*. Measurement of the equal-time correlations between the force at the wall and local fluctuations in the flow velocity at various points in the flow are strongly anisotropic: these correlations die off extremely rapidly in the direction of the flow, but span the entire width of the flow in the transverse direction. This is indicative of transient collisional force chains that extend across the hopper, arresting the flow briefly before breaking up and allowing the flow to resume. These collision chains have been observed in simulations of frictionless grains (Ferguson *et al.* 2004).

The unequal-time correlation between force and velocity reveals that these correlations are carried up the flow very rapidly, at speeds comparable to the speed of sound in the material. Thus, a fluctuation in the wall force due to a local, thin, transient collision chain can produce a suppression in the flow velocity over a large region in the flow. We show in figure 9 that this length scale grows as the flow is brought closer to jamming. A similar growth in length scale has been observed in two-dimensional simulations of flows (Tewari *et al.* 2009).

In a two-dimensional geometry, it is difficult to assess experimentally the significance of the confining walls in the formation of stress-bearing structures. In this section, we present new data that test the existence of force correlations in the thee-dimensional silo geometry of figure 1. As shown in figure 10, we attach two pairs of normal force transducers to the walls of the thee-dimensional silo with the transducers in a pair diametrically across from one another. The relative

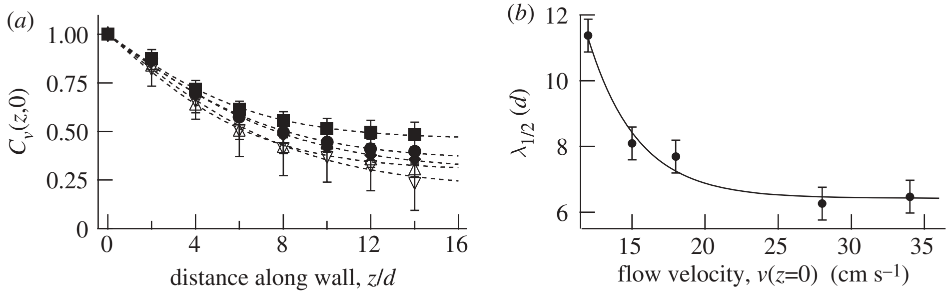

Figure 9. (a) Equal-time spatial cross-correlations $C_v(z, 0)$ between fluctuations in flow speed v at different positions, z, along the wall of the two-dimensional hopper shown in figure 1a. Data are shown for five flow speeds v ranging from 12 to $34\,\mathrm{cm\,s^{-1}}$. (b) The distance, $\lambda_{1/2}$, at which the spatial correlation $C_v(z, 0)$ decays to 0.5, as a function of flow speed, v. After Gardel *et al.* (submitted).

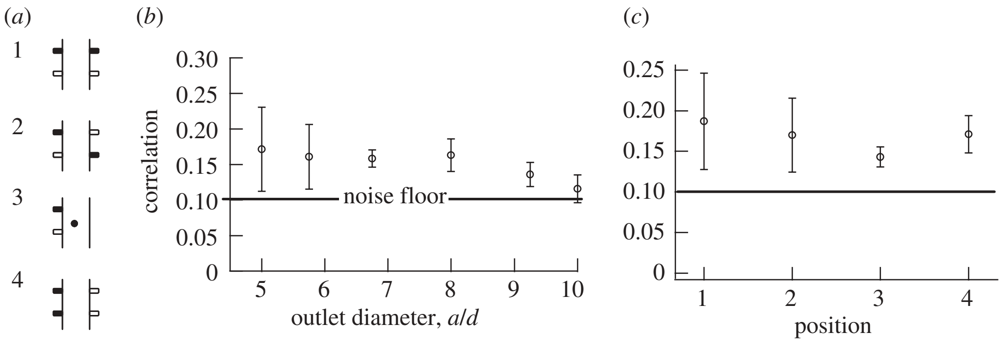

Figure 10. Two-point force correlations, $\langle \delta F_a \delta F_b \rangle / \sqrt{\langle \delta F_a^2 \rangle \langle \delta F_b^2 \rangle}$, where a and b label different transducers. (a) Four choices of spatial configurations of transducer pairs are shown. The two black transducers in each configuration are paired in the correlation function. (b) The equal-time correlation between diametrically opposed pairs of transducers for flow rates spanning the range of our experiment. The correlations are much smaller than observed in the two-dimensional hopper flow, but are statistically significant. The noise level is determined by correlating time series from two different runs. (c) The equal-time correlation at a fixed flow rate, between different spatial configurations of transducer pairs. The numerical index on the horizontal axis corresponds to the four configurations shown on the left.

orientation of the diameters connecting the two pairs can be varied; here we report on results in configurations with the diameters either parallel or perpendicular to each other. The transducer voltages are acquired at 80 kHz and converted to forces, as discussed in §2.

Having multiple transducers allows us to measure directly the correlations in force between a pair of points in space located at any two of the four transducers. It must of course be recognized that, if the force fluctuations are organized along long, thin structures, then the probability that a collision chain emanating from one wall at one transducer will terminate at a point on the wall where another transducer is located is small. However, as shown in figure 10b, there is a small,

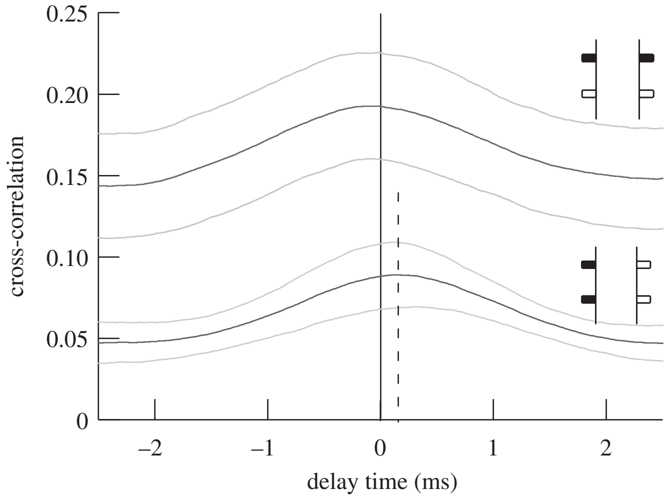

Figure 11. Unequal-time two-point force correlations, $\langle \delta F_a(0)\delta F_b(t)\rangle/\sqrt{\langle \delta F_a^2\rangle\langle \delta F_b^2\rangle}$, for two different transducer configurations. The upper curve, which is for diametrically opposed transducers, peaks at $t=0$, whereas the lower curve, which is for two vertically displaced transducers, peaks at a finite positive time, indicating that correlations are transported up the flow. The grey curves indicate standard deviations.

but statistically significant positive correlation between the force experienced by transducers across the diameter of the silo. These correlations do not appear to be dependent on the flow speed.

Moreover, the magnitude of the correlation is not dependent on the relative orientation of the pair of transducers used to construct the correlation, as shown in figure 10*c*. There are two possible interpretations of this observation. One is that the force fluctuations in three-dimensional flows are not organized in local structures. The other is that local fluctuations are propagated very quickly in space. We present in figure 11 the evidence of this time delay. Unequal-time correlations of the force between two diametrically opposed transducers peak at zero time, indicating that, on average, force fluctuations at these two points coincide in time. The force correlations between two transducers displaced from each other in the flow direction, however, occur at a finite time delay. The sign of the time delay indicates that the fluctuations are propagated upwards, in the direction against the flow. From the distance between the transducers and the time delay, we can compute the speed at which the correlations propagate. This speed is considerably higher than the flow velocity, and increases as the flow velocity is decreased towards jamming. For the example shown in figure 11 with a flow velocity of $0.053\,\mathrm{m\,s^{-1}}$, this speed is $151\,\mathrm{m\,s^{-1}}$. For a higher flow velocity of $0.23\,\mathrm{m\,s^{-1}}$, this speed is $92\,\mathrm{m\,s^{-1}}$. The correlation speeds are comparable to the sound speeds measured in granular media, and this speed increases as jamming is approached.

Thus the flowing medium shows increasingly solid-like behaviour, in terms of its response to high-frequency fluctuations. We are not able to determine from our data whether the local fluctuations are organized in one-dimensional chains as in the two-dimensional hopper or whether two-dimensional structures are developed in a three-dimensional flow. That is to say, the absence of directionality exhibited in figure 10*c* is consistent both with arch-like and vault-like structures.

6. Discussion

We have thus studied, by measurements of wall forces and kinematics, a regime of dense flow close to the jamming transition in a variety of flow geometries. The microscopic picture that emerges from studying the flow at the grain scale, and at a fast temporal resolution, shows a continuous, but marked, evolution from entirely collisional dynamics to frictional dynamics as the jamming transition is approached.

When this microscopic state is coarse grained in time to time scales that are barely above the mean free time, several features of the flow become independent of flow velocity. Despite the vastly different underlying micromechanics, the probability distribution of force, the mean 'friction angle' and the correlation between the force components are all essentially independent of the flow velocity. However, it is not correct to conceive of this state of the system as quasi-static, since several time-dependent features of the flow do not merely scale with the flow velocity. Both the amplitude of the fluctuations and their frequency spectrum change with flow velocity even well below the characteristic frequency of collisions. Given this, it is somewhat puzzling that some important macroscopic features of the system are independent of flow speed.

As the threshold to jamming is approached, the fluctuations also become more correlated, and the length scale associated with velocity fluctuations rapidly increases. In this respect, flowing systems are different from randomly agitated granular systems, in which the approach to jamming manifests itself much more subtly—with correlation lengths of a few particle diameters that can only be captured by higher-order correlation functions (Dauchot *et al.* 2005; Keys *et al.* 2007). The force fluctuations that generate velocity fluctuations are local in character. In two dimensions they are highly anisotropic, chain-like structures. In three dimensions they are also local, but their geometry has not yet been clarified. However, these local structures have significant non-local consequences—the effects of a large force fluctuation are propagated upwards in the flow at propagation speeds comparable to the speed of sound in the material. These propagation speeds also increase as the jamming threshold is approached.

It appears that visco-plastic models that were designed for steady flows away from jamming do not fully capture the correlated, non-local character of this flow, nor do rapid flow theories based on kinetic theories, even though the flows can be largely collisional in this regime. It remains an open question as to what the right framework is for describing the state of flow that is close to arrest.

We acknowledge financial support from the National Science Foundation via NSF-DMR 0606216 and the MRSEC on Polymers at the University of Massachusetts. We are also grateful for helpful input from T. J. Schicker, A. Stratulat and S. Tewari.

References

Beverloo, W. A., Leniger, H. A. & van der Welde, J. 1961 The flow of granular solids through orifices. *Chem. Eng. Sci.* **15**, 260. (doi:10.1016/0009-2509(61)85030-6)

Dauchot, O., Marty, G. & Biroli, G. 2005 Dynamical heterogeneity close to the jamming transition in a sheared granular material. *Phys. Rev. Lett.* **95**, 265701. (doi:10.1103/PhysR3vLett.95.265701)

Ertas, D. & Halsey, T. C. 2002 Granular gravitational collapse and chute flow. *Europhys. Lett.* **60**, 931–937. (doi:10.1209/epl/i2002-00307-8)

Ferguson, A., Fisher B. & Chakraborty, B. 2004 Impulse distributions in dense granular flows: signatures of large-scale spatial structures. *Europhys. Lett.* **66**, 277–283. (doi:10.1209/epl/i2003-10190-3)

Forterre, Y. & Pouliquen, O. 2008 Flows of dense granular media. *Annu. Rev. Fluid Mech.* **40**, 1–24. (doi:10.1146/annurev.fluid.40.111406.102142)

Gardel, E., Keene, E., Dragulin, S., Easwar, N. & Menon, N. Submitted. Force–velocity correlations in a dense, collisional, granular flow. (http://arxiv.org/abs/cond-mat/0601022)

GDR MiDi 2004 On dense granular flows. *Eur. Phys. J. E* **14**, 341–365.

Isa, L., Besseling, R. & Poon, W. C. K. 2007 Shear zones and wall slip in the capillary flow of concentrated colloidal suspensions. *Phys. Rev. Lett.* **98**, 198305. (doi:10.1103/PhysRevLett.98.198305)

Keys, A. S., Abate, A. R., Glotzer, S. C. & Durian, D. J. 2007 Measurement of growing dynamical length scales and prediction of the jamming transition. *Nat. Phys.* **3**, 260–264. (doi:10.1038/nphys.572)

Knight, J. B., Ehrichs, E. E., Kuperman, V. Y., Flint, J. K., Jaeger, H. M. & Nagel, S. R. 1997 Experimental study of granular convection. *Phys. Rev. E* **54**, 5726–5738. (doi:10.1103/PhysRevE.54.5726)

Longhi, E. C., Easwar, N. & Menon, N. 2002 Large force fluctuations in a flowing granular medium. *Phys. Rev. Lett.* **89**, 045501. (doi:10.1103/PhysRevLett.89.045501)

Losert, W., Bocquet, L., Lubensky, T. C. & Gollub, J. P. 2000. Particle dynamics in sheared granular matter. *Phys. Rev. Lett.* **85**, 1428–1431. (doi:10.1103/PhysRevLett.85.1428)

Menon, N. & Durian, D. J. 1997 Diffusing-wave spectroscopy of dynamics in a three-dimensional granular flow. *Science* **275**, 1920–1923. (doi:10.1126/science.275.5308.1920)

Mueth, D. M., Jaeger, H. M. & Nagel, S. R. 1998 Force distribution in a granular medium. *Phys. Rev. E* **57**, 3164–3169. (doi:10.1103/PhysRevE.57.3164)

Mueth, D. M., Debregeas, G. F., Karczmar, G. S., Eng, P. J., Nagel, S. R. & Jaeger, H. M. 2000 Signatures of granular microstructure in dense shear flows. *Nature* **406**, 385–389. (doi:10.1038/35019032)

Pouliquen, O. 1999 Scaling laws in granular flows down rough inclined planes. *Phys. Fluids* **11**, 542–548. (doi:10.1103/PhysRevE.53.552)

Pouliquen, O. & Gutfraind, R. 1996 Stress fluctuations and shear zones in quasistatic granular chute flows. *Phys. Rev. E* **53**, 552. (doi:10.1063/1.869928)

Silbert, L. E., Ertas, D., Grest, G. S., Halsey, T. C., Levine, D. & Plimpton, S. J. 2001 Granular flow down an inclined plane: Bagnold scaling and rheology. *Phys. Rev. E* **64**, 051302. (doi:10.1103/PhysRevE.64.051302)

Tewari, S., Tithi, B., Ferguson A. & Chakraborty, B. 2009 Growing length scale in gravity-driven dense granular flow. *Phys. Rev. E* **79**, 0011303. (doi:10.1103/PhysRevE.79.0011303)